Mechanism and Thermochemistry of Peroxynitrite Decomposition in Water

Gábor Merényi,*,† Johan Lind,† Sara Goldstein,‡ and Gidon Czapski‡

Department of Chemistry, Nuclear Chemistry, The Royal Institute of Technology, S-10044 Stockholm 70, Sweden, and Department of Physical Chemistry, The Hebrew University of Jerusalem, Jerusalem 91904, Israel

Received: December 9, 1998; In Final Form: April 19, 1999

The formation of ONOOH/$ONOO^-$ in water has been studied using the pulse radiolysis of nitrite and nitrate solutions. The overall rate constant of the reaction of $^\bullet OH$ with $^\bullet NO_2$ was determined to be $(1.0 \pm 0.2) \times 10^{10}$ M^{-1} s^{-1}. This reaction generates almost equal amounts of ONOOH and $NO_3^- + H^+$. The overall rate constant of the reaction of $^\bullet NO_2$ with $O^{\bullet -}$ was determined to be $(3-4) \times 10^9$ M^{-1} s^{-1}. From published thermodynamic data the equilibrium constant of homolysis of $ONOO^-$ into $^\bullet NO_2$ and $O^{\bullet -}$ is calculated to be $(5.9 \pm 2.9) \times 10^{-16}$ M, and hence the calculated rate constant of homolysis of $ONOO^-$ into $^\bullet NO_2$ and $O^{\bullet -}$ is $(0.9-3.5) \times 10^{-6}$ s^{-1}. The rate constants for $ONOO^-$ decomposition at pH 13 and 14 (25 °C) were determined to be 1.3×10^{-5} and 1.1×10^{-5} s^{-1}, respectively, and the yield of NO_2^- in this process was found to be ca. 50%. On the assumption that ca. 1/2 of $ONOO^-$ decomposes via homolysis into $^\bullet NO_2$ and $O^{\bullet -}$, a limiting rate constant for the decomposition of $ONOO^-$ can be predicted at sufficiently high pH, $k_d = (0.36-1.4) \times 10^{-5}$ s^{-1}, which is four times as high as the rate constant of homolysis into $^\bullet NO_2$ and $O^{\bullet -}$. Both results are in excellent agreement with the homolysis model. The activation parameters for the decomposition of $ONOO^-$ at pH 14 were determined to be $A = 8 \times 10^{10}$ s^{-1} and $E_a = 21.7$ kcal/mol. The relatively low A value suggests a high degree of solvent organization in the transition state. The mechanisms of homolysis of ONOOH and $ONOO^-$ are compared and discussed in detail.

Introduction

The importance of the coupling of $^\bullet NO$ with $O_2^{\bullet -}$ to yield $ONOO^-$ in biological systems was first suggested by Beckman et al.[1] Using different methods, the rate constant of this reaction has been determined to be between 3.8×10^9 and 1.9×10^{10} M^{-1} s^{-1}.[2-6] The rate of decomposition of peroxynitrite (ONOOH/$ONOO^-$) is highly pH-dependent, and it has been suggested that only the acid form, ONOOH, decomposes ($k_o = 1.2-1.3$ s^{-1} at 25 °C),[5,7] whereas $ONOO^-$ is essentially stable.[5,7] The pK_a(ONOOH) = 6.5−6.8 has been determined using kinetics[5,7] and absorption[3,8] measurements. However, it has been reported in several earlier studies[9-14] that the measured decay rates of $ONOO^-$ at pH > 10 are faster than the calculated ones assuming that only the acidic form decomposes. An exceptional situation arises when CO_2 (added or adventitious) accelerates $ONOO^-$ decomposition[15] and gives rise to very reactive intermediates during this process.[16,17]

The decomposition of peroxynitrite in acidic solutions mainly yields nitrate as the final product, but as the pH is raised, O_2 and nitrite in a 1:2 proportion are formed at the expense of nitrate, reaching ca. 40% O_2 at pH 9.[18,19] The mechanism of the decomposition of peroxynitrite has been under controversy.[5,7,20-22] However, in our opinion, this controversy is now resolved in its major points, as a scrutiny of ref 23 will reveal. It has been shown that the pH dependence of the product yield during peroxynitrite decomposition is explained by the simultaneous presence of homolysis reactions 1 and 2.[24] As $k_2 \approx 0.02$ s^{-1} and the effective rate constant of reaction 1 decreases above

$$ONOOH \rightleftharpoons {}^\bullet NO_2 + {}^\bullet OH \quad (1)$$

$$ONOO^- \rightleftharpoons {}^\bullet NO + O_2^{\bullet -} \quad (2)$$

pK_a(ONOOH), the contribution to the product yield of reaction 2 relative to that of reaction 1 increases with pH and becomes dominant above pH 8.[24] Therefore, the experimental yields of nitrite and O_2 increase with pH at the expense of the nitrate in a sigmodial fashion, and the two yields become roughly equal at ca. pH 8,[19] which differs from pK_a(ONOOH).

Koppenol and co-workers argued against homolysis (reaction 1)[22,25,26] as, in their interpretation of the data in ref 8, homolysis would be followed by rapid recombination of $^\bullet NO_2$ with $^\bullet OH$ to yield mainly ONOOH.[26] This reasoning, however, is not correct, because the highly reactive and unselective $^\bullet OH$ radical would react predominantly with nitrite, peroxynitrite, the buffer or impurities, and thus less than ca. 1% of it would recombine with $^\bullet NO_2$. Furthermore, we shall show in the present study, for the first time, that the reaction of $^\bullet OH$ with $^\bullet NO_2$ generates almost equal amounts of ONOOH and $NO_3^- + H^+$.

Recently, the Gibbs free energy of formation of $ONOO^-$ in water was determined to be 16.6 ± 0.4 kcal/mol,[24] and from this value and other thermodynamic data the equilibrium constant of reaction 3 can be obtained.

$$ONOO^- \rightleftharpoons {}^\bullet NO_2 + O^{\bullet -} \quad (3)$$

As a consequence of reaction 3 the decay rate of $ONOO^-$ at sufficiently high pH must reach a lower limit. Part of these results has been presented in ref 27. The present work gives, among others, a detailed description of the prediction and determination of this limiting rate constant. Furthermore, the

* To whom all correspondence should be directed.
† Royal Institute of Technology.
‡ Hebrew University of Jerusalem.

10.1021/jp984686h CCC: $18.00 © 1999 American Chemical Society
Published on Web 07/02/1999

TABLE 1: Reaction Mechanism and Rate Constants for the Nitrite System Where Only Reactions −1, 4−6, and 9−11 Were Used for Simulating Peroxynitrite Yields

no.	reaction	k, M^{-1} s^{-1}	ref
4	$^{\bullet}OH + NO_2^- \rightarrow OH^- + {}^{\bullet}NO_2$	$(5.3 \pm 0.5) \times 10^9$	this work (33)
5	$^{\bullet}OH + {}^{\bullet}OH \rightarrow H_2O_2$	5.5×10^9	32
6	$^{\bullet}OH + ONOO^- \rightarrow ONOO^{\bullet} + OH^-$ $(NO + O_2 + OH^-)$	4.8×10^9	35[a]
−1	$^{\bullet}OH + {}^{\bullet}NO_2 \rightarrow ONOOH$	$(4.5 \pm 1.0) \times 10^9$	this work
7	$^{\bullet}NO_2 + {}^{\bullet}NO_2 \rightleftharpoons N_2O_4$	$k_7 = 4.5 \times 10^8$ $k_{-7} = 6.9 \times 10^3$ s^{-1}	36
8	$N_2O_4 + H_2O \rightarrow NO_2^- + NO_3^- + 2H^+$	18.0	36
9	$H^{\bullet} + {}^{\bullet}NO_2 \rightarrow NO_2^- + H^+$	1×10^{10}	8
10	$H^{\bullet} + {}^{\bullet}OH \rightarrow H_2O$	2×10^{10}	37
11	$H^{\bullet} + NO_2^- \rightarrow {}^{\bullet}NO + OH^-$	7.1×10^8	32
	$ONOOH \rightleftharpoons ONOO^- + H^+$	$pK_a = 6.6$	3, 5, 8

[a] A referee suggested that reaction 6 may instead be an oxygen transfer, yielding NO_2^- and $HO_2^{\bullet}$. Experimentally, these two possibilities are indistinguishable, since both reaction modes will result in the same final product distribution. However, we feel that electron transfer is more likely than oxygen transfer, as the latter reaction is expected to be slower than the former. For instance, even the energetically extremely favorable oxygen transfer reaction between $^{\bullet}OH$ and O_3 has a rate constant as low as 10^8 M^{-1} s^{-1}.[32]

temperature dependence of the decay rate of $ONOO^-$ will be reported and compared to that of ONOOH.

Experimental Section

Chemicals. All chemicals were of analytical grade and were used as received. Solutions were prepared with distilled water that was further purified using a Milli-Q water purification system. Fresh solutions of peroxynitrite were prepared daily by reacting nitrite with acidified hydrogen peroxide at room temperature in a quenched-flow system, as was recently described.[28] The yield of $ONOO^-$ was determined from its absorption at 302 nm using $\epsilon = 1670$ M^{-1} cm^{-1}.[29] The stock solution of peroxynitrite contained 7−9% nitrite and practically no residual H_2O_2.

Apparatus. Stopped-flow kinetic measurements were carried out using the Bio SX-17MV Sequential Stopped-Flow from Applied Photophysics with a mixing time of less than 2 ms and a 1 cm long mixing cell. The peroxynitrite ion at pH 12 was mixed in a 1:1 ratio with 0.2 M acetate buffer to a final pH of 4, which was measured at the outlet of the flow system. The decomposition of ONOOH was followed at 280 nm. The kinetic measurements were carried out at 3.2−48.1 °C.

The decomposition of $ONOO^-$ was followed at 302 nm in closed cuvettes to eliminate the absorption of CO_2 by the solution, which may interfere with the measurements. The kinetic measurements were carried out at 25−77 °C using a HP 8452A diode array spectrophotometer coupled with a thermostat (HP 89075C Programmable Multicell Transport).

Pulse radiolysis experiments at ambient temperature were carried out in Stockholm with a 3 MeV linear accelerator using a pulse length of 6 ns. Doses ranged from 16 to 26 Gy/pulse. The computerized optical detection system has been described elsewhere.[30] Corresponding experiments in Jerusalem were run with a Varian 7715 linear accelerator with 5 MeV electron pulses of 1.5 μs and 200 mA, as previously described in detail.[3] Dosimetry was performed with a N_2O-saturated 5 mM $K_4Fe(CN)_6$,[31] and doses ranged from 39 to 43 Gy/pulse. Briefly, irradiation of He-saturated aqueous solutions generates essentially equal amounts of $^{\bullet}OH$ and e_{aq}^-, and the latter is converted into $^{\bullet}OH$ when He is replaced by N_2O. In both systems the yield of $H^{\bullet}$ is ca. 10% of the total radical yield at pH > 3, and at pH 14 $H^{\bullet}$ is converted into e_{aq}^- via its reaction with OH^-.[32]

Modeling of the experimental results was carried out using INTKIN, a noncommercial program developed at Brookhaven National Laboratories by Dr. H. A Schwarz.

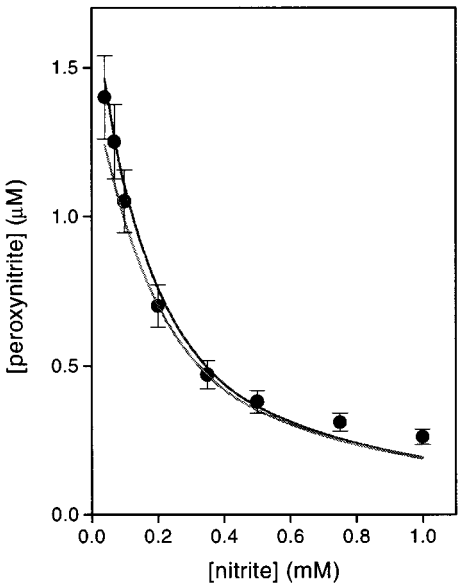

Figure 1. Experimental (±10%) and modeled (solid lines) yields of peroxynitrite measured in irradiated N_2O-saturated solutions as a function of nitrite concentration at pH 8, 20 ms after a constant pulse of 37 Gy. The upper line was obtained with $k_{-1} = 4.5 \times 10^9$ M^{-1} s^{-1} and $k_{-1a} = 0$; the lower line, with $k_{-1} = 4.5 \times 10^9$ M^{-1} s^{-1}, $k_{-1a} = 3.5 \times 10^9$ M^{-1} s^{-1}.

Results

Reaction of $^{\bullet}OH$ with $^{\bullet}NO_2$. Previously, the rate constant of reaction −1 has been determined to be $(4.5 \pm 1.0) \times 10^9$ M^{-1} s^{-1} using pulse radiolysis of N_2O-saturated nitrite solutions at pH 9.5.[8] In the present study additional pulse-radiolysis experiments were performed, where the yield of peroxynitrite was measured as a function of $[NO_2^-]_o$ at pH 8.0 (2 mM phosphate buffer) for a pulse of 37 Gy (Figure 1). Under these conditions the formation of peroxynitrite via reaction −1 is affected by other second-order radical−radical reactions as well as by reactions involving the $H^{\bullet}$ radical, which makes up 10% of the total radical yield. The reaction mechanism for this system is given in Table 1. The absorption at 302 nm was measured 20 ms after the pulse, where the excess of $^{\bullet}NO_2$ and N_2O_4, which are formed in this system and absorb in the same wavelength region as $ONOO^-$, have already decayed (reactions 7 and 8). The rate constant of the reaction of $^{\bullet}OH$ with N_2O_4 is not known. However, even if it were to approach the diffusion-controlled limit, the contribution of this reaction would be minor, and hence can be ignored. The reported values of k_4 vary in the literature

TABLE 2: Reaction Mechanism and Rate Constants Used for Simulating Peroxynitrite Yields in the Nitrate System

no.	reaction	k, M^{-1} s^{-1}	ref
12	$e_{aq}^- + NO_3^- \rightarrow NO_3^{2-}$	9.7×10^9	33
13	$NO_3^{2-} + H_2O \rightarrow {}^\bullet NO_2 + 2OH^-$	5.5×10^4	8, 39
13a	$NO_3^{2-} + H_2PO_4^- \rightarrow {}^\bullet NO_2 + HPO_4^{2-} + OH^-$	5×10^8	39[a]
5	${}^\bullet OH + {}^\bullet OH \rightarrow H_2O_2$	5.5×10^9	32
6	${}^\bullet OH + ONOO^- \rightarrow {}^\bullet NO + O_2 + OH^-$	4.8×10^9	34
−1	${}^\bullet OH + {}^\bullet NO_2 \rightarrow ONOOH$	$(4.5 \pm 1.0) \times 10^9$	this work
−1a	${}^\bullet OH + {}^\bullet NO_2 \rightarrow NO_3^- + H^+$	$(4.5 \pm 1.0) \times 10^9$	this work
7	${}^\bullet NO_2 + {}^\bullet NO_2 \rightleftharpoons N_2O_4$	$k_7 = 4.5 \times 10^8$ $k_{-7} = 6.9 \times 10^3$ s^{-1}	36
8	$N_2O_4 + H_2O \rightarrow NO_2^- + NO_3^- + 2H^+$	18.0	36
9	$H^\bullet + {}^\bullet NO_2 \rightarrow NO_2^- + H^+$	1×10^{10}	8
10	$H^\bullet + {}^\bullet OH \rightarrow H_2O$	2×10^{10}	37
14	$H^\bullet + NO_3^- \rightarrow HNO_3^-$	1.0×10^7	8
	$ONOOH \rightleftharpoons ONOO^- + H^+$	$pK_a = 6.6$	3, 8, 5

[a] The rate of conversion of NO_3^{2-} into ${}^\bullet NO_2$ is catalyzed by $H_2PO_4^-$, and under our experimental conditions (4−10 mM phosphate buffer, pH 5.6−8) the rate constant for this process exceeds 1×10^6 s^{-1}.[8,38]

from 6.0×10^9 to 1.4×10^{10} M^{-1} s^{-1}.[32] Therefore, we redetermined $k_4 = (5.3 \pm 0.5) \times 10^9$ M^{-1} s^{-1} under our experimental conditions (pH 8.0, 2 mM phosphate buffer) using competition kinetics with $Fe(CN)_6^{4-}$.[33] Reactions 7 and 8 were omitted from the simulation, as they have only a minor effect on the yield. Thus, only reactions −1, 4−6, and 9−11 (Table 1) were used for simulating peroxynitrite yields in the nitrite system. The best fit to the experimental results was obtained for $k_{-1} = (4.5 \pm 1.0) \times 10^9$ M^{-1} s^{-1} (Figure 1, upper line). Simulating both k_4 and k_{-1} and assuming $k_4 > 5.3 \times 10^9$ M^{-1} s^{-1} results in the best fit for $k_4 = 7 \times 10^9$ M^{-1} s^{-1} and $k_{-1} = 5.5 \times 10^9$ M^{-1} s^{-1}, where the former value is identical to that determined recently via competition with $IrCl_6^{3-}$.[34] The data could not be well fitted for $k_4 > 7 \times 10^9$ M^{-1} s^{-1}. Logager and Sehested[8] determined through simulation $k_{-1} = (4.5 \pm 1.0) \times 10^9$ M^{-1} s^{-1} and $k_4 = (6.0 \pm 1.0) \times 10^9$ M^{-1} s^{-1}, although reactions 6, 10, and 11 were ignored and both k_{-1} and k_4 were simulated (see ref 38). In the nitrite system the yield of peroxynitrite per ${}^\bullet OH$ radical is less than 10%, as most of the ${}^\bullet OH$ radicals are consumed in reactions 4 and 5. Since the product of reaction −1 is measured directly at 302 nm, k_{-1} can be determined accurately. In contrast, this system is unsuitable for the determination of k_{-1a}, given that direct observation of NO_3^- is not possible.

$$^\bullet OH + {}^\bullet NO_2 \rightarrow NO_3^- + H^+ \qquad (-1a)$$

In Figure 1 it is shown that the calculated lines for $k_{-1} = 4.5 \times 10^9$ M^{-1} s^{-1} and $k_{-1a} = 0$ or 3.5×10^9 M^{-1} s^{-1} fit the experimental yields almost equally well. We conclude that from the nitrite system one obtains $k_{-1} = (5.0 \pm 1.0) \times 10^9$ M^{-1} s^{-1}

For a reliable determination of k_{-1a} we have to study a system where the yield of ONOOH per ${}^\bullet OH$ radical is high, i.e., where reactions −1 and −1a are dominant processes. We therefore measured the yield of peroxynitrite as a function of pH in He-saturated solutions containing 3 mM nitrate and 4−10 mM phosphate buffer for a pulse of 43 Gy. The reaction mechanism is given in Table 2, where all rate constants are known except k_{-1a}. In this system one generates essentially equal amounts of ${}^\bullet OH$ and ${}^\bullet NO_2$ radicals, and the yield of ONOOH per ${}^\bullet OH$ radical is substantially higher than in the nitrite system, because the ${}^\bullet OH$ radicals are consumed at comparable rates in reactions −1 and 5. Figure 2 displays the experimental and simulated yields of peroxynitrite at different pH values for $k_{-1} = 5 \times 10^9$ M^{-1} s^{-1} and $k_{-1a} = 0$, 5×10^9, and 7×10^9 M^{-1} s^{-1}. As seen from this figure, exclusion of reaction −1a in the simulation results in considerably higher calculated peroxynitrite yields than

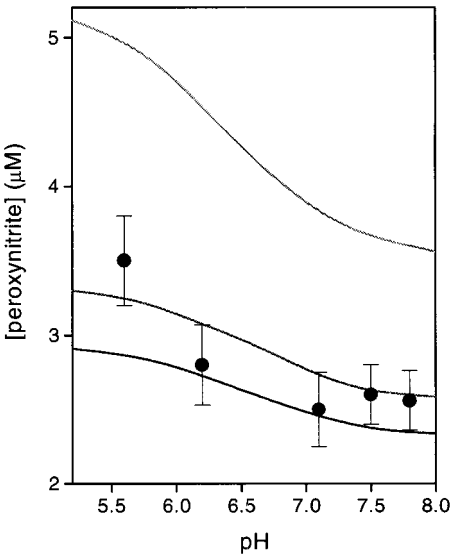

Figure 2. Experimental (±10%) and modeled (solid lines) yields of peroxynitrite measured in irradiated He-saturated solutions containing 3 mM nitrate as a function of pH, 20 ms after a constant pulse of 43 Gy. All lines were calculated with $k_{-1} = 5 \times 10^9$ M^{-1} s^{-1} and $k_{-1a} = 0$ (upper), 5×10^9 M^{-1} s^{-1} (middle), and 7×10^9 M^{-1} s^{-1} (lower).

the experimental ones. The important conclusion is that, no matter what the precise value of k_{-1}, the best fit is obtained for $k_{-1} \approx k_{-1a}$. Therefore, the reaction of ${}^\bullet OH$ with ${}^\bullet NO_2$ generates about equal amounts of ONOOH and $NO_3^- + H^+$. The overall rate constant of the recombination, $k_{-1} + k_{-1a}$, is $(1.0 \pm 0.2) \times 10^{10}$ M^{-1} s^{-1}.

Previously,[8] the yields of peroxynitrite were measured in the nitrate system only in acidic solutions (pH 0−3.85), and the modeled yields were reported to be identical to the measured ones assuming $k_{-1} = 4.5 \times 10^9$ M^{-1} s^{-1} and $k_{-1a} = 0$ (see our comments regarding these results in ref 40).

Reaction of $O^{\bullet -}$ with ${}^\bullet NO_2$. The effective rate constant of the reaction of ${}^\bullet OH/O^{\bullet -}$ with NO_2^- at pH 14 was found to be $(6.7 \pm 1.0) \times 10^7$ M^{-1} s^{-1} using competition kinetics with O_2 for which $k(O^{\bullet -} + O_2) = 3.6 \times 10^9$ M^{-1} s^{-1}.[32] This effective rate constant implies that more than 50% of the reaction is by way of ${}^\bullet OH$ reacting with NO_2^- to yield ${}^\bullet NO_2$. The formation of ${}^\bullet NO_2$ in the latter process was confirmed at pH 12 in irradiated N_2O-saturated solutions containing 2 mM NO_2^- and 0.4 mM methyl viologen (MV^{2+}). If $HNO_3^{\bullet -}$ were formed in the reaction of ${}^\bullet OH$ with NO_2^- at pH 12, the deprotonation of HNO_3^- by OH^- would be faster than the expulsion of OH^- from HNO_3^-,

TABLE 3: Reaction Mechanism and Rate Constants Used for Simulating the Yields of $ONOO^-$ and O_2NOO^- at pH 14

no.	reaction	k, M^{-1} s^{-1}	ref
15	$^{\bullet}OH + NO_2^- \rightarrow OH^- + {}^{\bullet}NO_2$	$k_{eff} = 6.7 \times 10^7$	this work
16	$O^{\bullet-} + O^{\bullet-} \rightarrow O_2^{2-}$	$\leq 9 \times 10^8$	32
−3	$^{\bullet}NO_2 + O^{\bullet-} \rightarrow ONOO^-$	$(3-4) \times 10^9$	this work
−3a	$^{\bullet}NO_2 + O^{\bullet-} \rightarrow NO_3^-$	$\leq 4 \times 10^9$	this work
17	$O^{\bullet-} + HO_2^- \rightarrow O_2^{\bullet-} + OH^-$	5.5×10^8	32
18	$^{\bullet}NO_2 + O_2^{\bullet-} \rightleftharpoons O_2NOO^-$	$k_{20} = 4.5 \times 10^9$ $k_{-20} = 1.0\ s^{-1}$	41, 42
19	$O_2NOO^- \rightarrow O_2 + NO_2^-$	$1.0\ s^{-1}$	41, 42

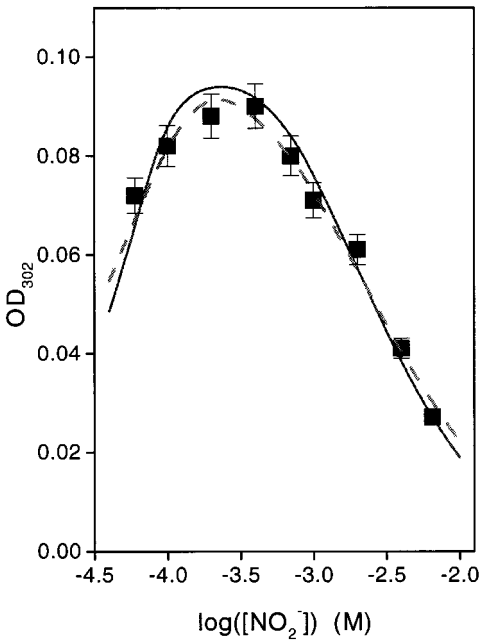

Figure 3. Experimental (±5%) and modeled (line) absorption yield measured at 302 nm in irradiated N_2O nitrite solutions at pH 14 as a function of nitrite concentration. The absorption was measured 4−10 ms after a constant pulse for which $[O^{\bullet-}] = 22\ \mu M$, where both $ONOO^-$ and O_2NOO^- absorb ($\epsilon_{302}(ONOO^-) = 1670\ M^{-1}cm^{-1}$,[29] $\epsilon_{302}(O_2NOO^-) = 1360\ M^{-1}cm^{-1}$ [41,42]). The optical path length was 12.1. The solid line was obtained with $k_{-3} = 3 \times 10^9\ M^{-1}\ s^{-1}$ and $k_{16} = 9 \times 10^8\ M^{-1}\ s^{-1}$, and the dashed line, with $k_{-3} = k_{-3a} = 4 \times 10^9\ M^{-1}\ s^{-1}$ and $k_{16} = 3 \times 10^8\ M^{-1}\ s^{-1}$.

and the fast reduction of MV^{2+} by NO_3^{2-} would take place.[32] However, the characteristic absorption of MV^+ under these conditions was not observed. If $O^{\bullet-}$ also contributes to the reaction at pH 14, it is likely to oxidize NO_2^- to $^{\bullet}NO_2$ rather than add to NO_2^- to form NO_3^{2-}. This follows from our finding that in irradiated He-saturated solutions containing 0.1 M NO_2^- and 1 M NaOH, the characteristic absorption of NO_3^{2-} in the UV region[39] was not observed.

When N_2O-saturated solutions containing 0.06−6.5 mM nitrite and 1 M NaOH were irradiated, all the primary free radicals formed by the radiation were converted into $O^{\bullet-}$, and the buildup of the absorption at 302 nm was observed. The dynamics of the system is described by the reactions in Table 3. The absorption at 302 nm as a function of added nitrite was measured 4−10 ms after a constant pulse (Figure 3). At this wavelength both $ONOO^-$ and O_2NOO^- absorb, where the former is by far the major absorbing species. At high nitrite concentrations (right-hand side of Figure 3) only reactions 15, −3, and −3a are important. A good fit could be obtained as long as k_{-3a} did not exceed $4 \times 10^9\ M^{-1}\ s^{-1}$. The value of k_{-3} is insensitive to that of k_{-3a}. Varying the latter from 0 to $4 \times 10^9\ M^{-1}\ s^{-1}$ caused k_{-3} to increase from 3×10^9 merely to $4 \times 10^9\ M^{-1}\ s^{-1}$. Keeping k_{16} in the interval $(3-9) \times 10^8\ M^{-1}\ s^{-1}$, we can get a good fit over the whole nitrite concentration regime (Figure 3). We conclude that $k_{-3} = (3-4) \times 10^9\ M^{-1}\ s^{-1}$ and that the yield of NO_3^- formed in the reaction of $O^{\bullet-}$ with $^{\bullet}NO_2$ cannot exceed 50%.

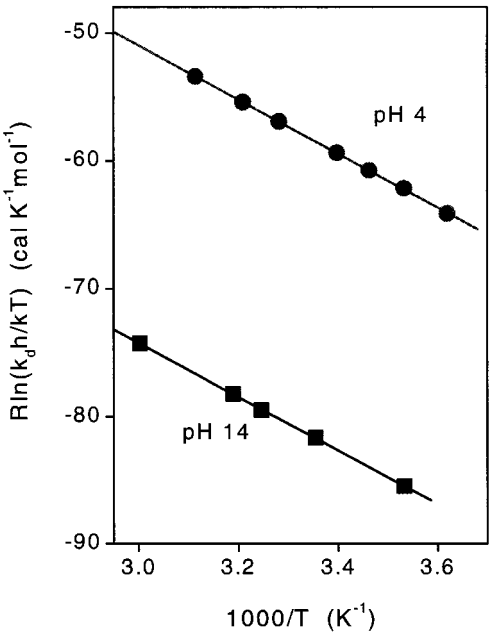

Figure 4. Eyring plots obtained for the decomposition of peroxynitrite at pH 4 and 14.

TABLE 4: Activation Parameters Obtained for the Decomposition of ONOOH and $ONOO^-$ at pH 4 and 14, Respectively

pH	$\Delta S^{\ddagger}$, eu	$\Delta H^{\ddagger}$, kcal/mol	E_a, kcal/mol	A, s^{-1}
4	13	21.2	21.8	1×10^{16}
14	−11	21.1	21.7	8×10^{10}

Decay of ONOOH at pH 4. The temperature dependence of the decomposition rate of ONOOH was measured in the interval 3.2−48.1 °C at pH 4 (0.1 M acetate buffer). The Eyring plot is given in Figure 4, and the extracted activation parameters are collected in Table 4.

Decay of $ONOO^-$ at High pH. The decomposition of 0.1−0.45 mM $ONOO^-$ at pH >12 obeyed first-order kinetics. The observed first-order rate constant was found to be independent of $[ONOO^-]_o$ (Figure 5), and hardly affected by the presence of 0.1 mM DTPA (results not shown). The latter observation rules out catalysis of $ONOO^-$ decomposition by traces of metal impurities, as suggested earlier.[14] The derived first-order rate constants at pH 12.2, 13, and 14 are very close, 2.1×10^{-5}, 1.3×10^{-5}, and $1.1 \times 10^{-5}\ s^{-1}$, respectively (Figure 5), and give the limiting rate constant $k_d \approx 1 \times 10^{-5}\ s^{-1}$ at 25 °C.

During the decomposition of peroxynitrite at pH 14 we observed the buildup of the characteristic absorption of nitrite (Figure 6). We determined the yield of nitrite between pH 13 and 14 using the Griess method to be ca. 50% at 25 °C (unpublished results).

The temperature dependence of the decomposition rate of $ONOO^-$ was measured in the interval 25−77 °C. The Eyring plot is given in Figure 4, and the extracted activation parameters are collected in Table 4.

Discussion

Yield of $^{\bullet}OH$ Radicals during Decomposition of ONOOH. It has been well established that the major product of ONOOH

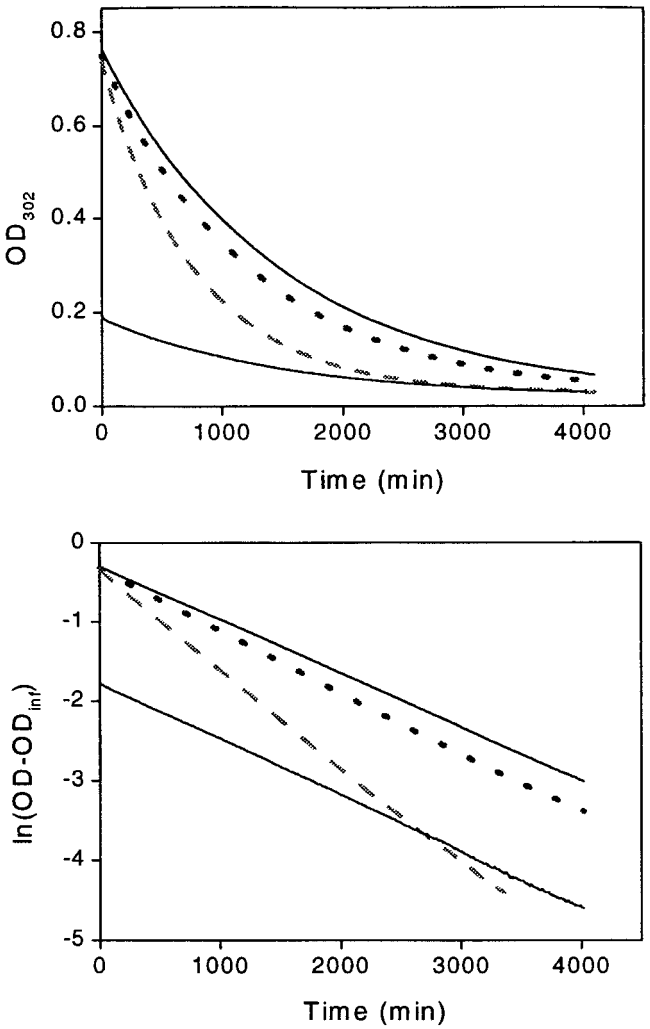

Figure 5. Decomposition at 25 °C of 0.46 mM $ONOO^-$ at pH 12.2 (dashed line, $k_d = 2.1 \times 10^{-5}$ s^{-1}), pH 13 (dotted line, $k_d = 1.3 \times 10^{-5}$ s^{-1}), and pH 14 (solid line, $k_d = 1.1 \times 10^{-5}$ s^{-1}). Lower solid line: decomposition of 0.11 mM $ONOO^-$ at pH 14, $k_d = 1.2 \times 10^{-5}$ s^{-1}.

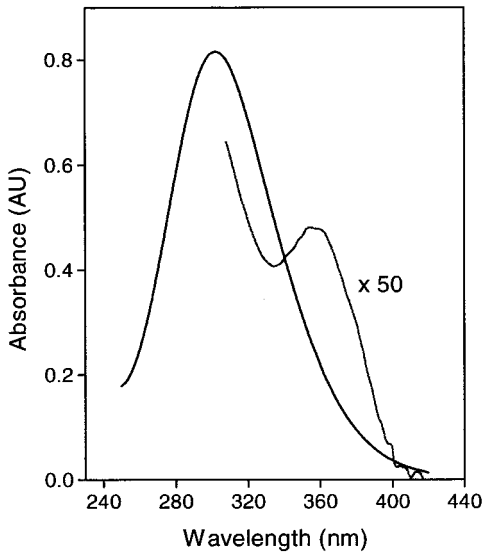

Figure 6. The absorption of 0.485 mM $ONOO^-$ at pH 14 after 22 h, where $ONOO^-$ was allowed to decay at 40.5 °C.

decomposition is NO_3^-.[14,18,19] There is also consensus that a certain fraction of ONOOH forms a reactive intermediate, which is capable of oxidizing a large variety of substrates.[7,14,20] Generally, oxidation of a substrate by this intermediate leads to the formation of reactive radicals, which undergo further reactions, especially with peroxynitrite itself.[43] Therefore, conventional analysis of some end product(s) is rarely a reliable measure of the initial yield of oxidative intermediates. The results are least ambiguous if this radical is relatively stable, and its yield can be measured in situ by some spectroscopic method. Accordingly, the most reliable values are obtained in the $Fe(CN)_6^{4-}$ and ABTS (2,2′-azinobis(3-ethylbenzothiazoline-6-sulfonic acid)) systems where $Fe(CN)_6^{3-}$ or $ABTS^{\bullet+}$ are easily measured, and it is in these systems that the highest oxidation yields are found, i.e., 30−40%.[20] We believe that the highest yields give the best values, as any secondary reactions can only lower the yield of any particular end product. While the ABTS and $Fe(CN)_6^{4-}$ systems are suitable for the determination of the yield of the intermediate, they are not selective and therefore cannot reveal the nature of this intermediate. Our experimentally derived thermokinetic data[24] suggest that this reactive intermediate is the couple $^{\bullet}OH$ and $^{\bullet}NO_2$, and its yield is 30−40%. Consequently, lesser yields reported can probably be attributed to further consumption of initially formed radical and nonradical products by $^{\bullet}NO_2$ and/or by secondary radicals formed from $^{\bullet}OH$ and the substrate.

Comparison of Predicted and Experimental k_d Values. The Gibbs free energy of formation of $ONOO^-$ in water has been determined to be $\Delta_f G°$ $(ONOO^-) = 16.6 \pm 0.4$ kcal/mol.[24] Utilizing $\Delta_f G°(^{\bullet}NO_2) = 15.1$ kcal/mol[44] and $\Delta_f G°(O^{\bullet-}) = 22.4$ kcal/mol,[44] we obtain $K_3 = (5.9 \pm 2.9) \times 10^{-16}$ M, and using $k_{-3} = (3-4) \times 10^9$ M^{-1} s^{-1}, one calculates $k_3 = (0.9-3.5) \times 10^{-6}$ s^{-1}.

The decomposition of $ONOO^-$ to yield NO_2^- and O_2 at pH 14 can be described by reactions 2, 3, 3a, and 20−23.

$$O^{\bullet-} + O_2 \rightleftharpoons O^{\bullet-}$$
$$k_{20} = 3.8 \times 10^9\ M^{-1}\ s^{-1},\ k_{-20} = 2.6 \times 10^3\ s^{-1}\ [45] \quad (20)$$

$$O_3^{\bullet-} + {}^{\bullet}NO \rightarrow NO_2^- + O_2$$
$$k_{21} = 3.5 \times 10^9\ M^{-1}\ s^{-1}\ [46] \quad (21)$$

$$^{\bullet}NO + {}^{\bullet}NO_2 \rightleftharpoons N_2O_3$$
$$k_{22} = 1.1 \times 10^9\ M^{-1}\ s^{-1},\ k_{-22} = 8.4 \times 10^3\ s^{-1}\ [39] \quad (22)$$

$$N_2O_3 + 2OH^- \rightarrow 2NO_2^- + H_2O$$
$$k_{23} = 1 \times 10^8[OH^-]\ s^{-1}\ [47] \quad (23)$$

As k_2 is much larger than k_3, the equilibrium between $ONOO^-$ and $^{\bullet}NO + O_2^{\bullet-}$ (reaction 2) is maintained throughout the decomposition of $ONOO^-$, and the equilibrium concentrations of $^{\bullet}NO$ and $O_2^{\bullet-}$ are in large excess (more than 1000-fold) over the steady state concentrations of $^{\bullet}NO_2$ and $O_3^{\bullet-}$. Thus, $^{\bullet}NO_2$ and $O_3^{\bullet-}$ will consume $O_2^{\bullet-}$ (reactions 18 and 19) and $^{\bullet}NO$ (reactions 21−23), and the net result is the consumption of two $ONOO^-$ ions for every homolysis via reaction 3. However, as during the decomposition of $ONOO^-$ the yield of NO_3^- is ca. 50%, it follows that $k_d = 2k_3 + k_{3a}$, $k_{3a}/(k_{3a} + 2k_3) \approx 0.5$, and hence $k_3 \approx 0.5k_{3a}$.

$$ONOO^- \rightarrow NO_3^- \quad (3a)$$

Thus, $k_d = 4k_3 = (0.36-1.4) \times 10^{-5}$ s^{-1}, which is in excellent agreement with the experimental limiting $k_d \approx 1 \times 10^{-5}$ s^{-1}. We conclude that the magnitude of k_d at high pH constitutes

SCHEME 1

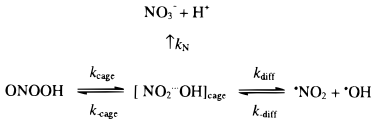

SCHEME 2

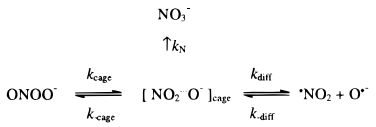

another strong evidence, were one more needed, for the homolysis reactions 1−3.

Description of Homolysis in Terms of the Radical Cage Model. The homolysis of chemical species into free radicals in any liquid solvent does not occur in one step, as in the gas phase at low pressures. Instead, the initial product of homolysis is a short-lived radical-pair cage with an average lifetime shorter than 1 ns.[48,49] The detailed mechanisms of homolysis reactions 1 and 3 are presented in Schemes 1 and 2. The radical-pair in the cage can (i) diffuse out of the cage into the bulk of the solution (k_{diff}), where the radicals are subject to thermodynamic solvation, and become what is called "free" radicals; (ii) collapse to form ONOOH in Scheme 1 or $ONOO^-$ in Scheme 2 by forming an O−O bond (k_{-cage}); (iii) collapse by forming a N−O bond, which results in the production of HNO_3 (immediately followed by dissociation into $NO_3^- + H^+$) in Scheme 1 and of NO_3^- in Scheme 2 (k_N). Applying the steady state approximation to the short-lived cage in Scheme 1, one obtains eq 24, where

$$k_o = k_{cage}(k_{diff} + k_N)/(k_{diff} + k_{-cage} + k_N) \qquad (24)$$

$k_N/k_{diff} \approx 2$ (30−40% oxidation yield) and $k_N/k_{-cage} \approx 1$ (the combination reaction of $^\bullet NO_2 + {}^\bullet OH$ yields approximately equal amounts of ONOOH and $NO_3^- + H^+$). Inserting these relationships, we obtain $k_o \approx 0.6k_{cage}$. To a good approximation, we can ascribe the activation energy of 21.8 kcal/mol (Table 4) to k_{cage}, and hence the frequency factor of k_{cage} would come out essentially the same as the experimental A value of 1×10^{16} s^{-1} (Table 4). The latter value is almost the same as 1.6×10^{16} s^{-1},[18] and close to 2×10^{15} s^{-1}, as reported recently.[26] This A value is of the same order of magnitude as those found for the homolysis of peroxides in the gas phase and in nonpolar organic solvents[50] and is a strong evidence for the validity of the radical-pair cage mechanism. Furthermore, it also reveals that the cage dynamics in water is not different from that in nonpolar solvents, suggesting that hydrogen bonding has little effect on the ratios of the microscopic rate constants.

The experimental rate constant for the decomposition of $ONOO^-$ according to Scheme 2 is given by eq 25.

$$k_d = 2k_3 + k_{3a} = k_{cage}(2k_{diff} + k_N)/(k_{diff} + k_{-cage} + k_N) \quad (25)$$

As the yield of NO_3^- during $ONOO^-$ decomposition at pH 14 is ca. 50%, it follows that $k_{diff}/k_N \approx 0.5$, which is similar to the homolysis of ONOOH. This suggests that k_{diff}/k_{-cage} may also be similar for $ONOO^-$ and ONOOH. However, our data on this point are not conclusive. The relatively low A factor (Table 4) of $ONOO^-$ homolysis must result from a strong solvation in the transition state implies structuring of water and thus a decreased entropy of activation. This contrasts to the "normal" frequency factor during homolysis of neutral species, where the change in solvation is much less dramatic.

Thermochemistry of ONOOH/$ONOO^-$ and $^\bullet OH/O^{\bullet -}$ in Aqueous Solution. The activation energy of ONOOH decomposition is 21.8 kcal/mol. We estimated $\Delta H^\circ = 19$ kcal/mol for reaction 1 assuming ca. 3 kcal/mol for the activation energy of the close to diffusion-controlled reverse reaction $k(^\bullet NO_2 + {}^\bullet OH)$. An independent estimate of ΔH°_1 can be made as follows. $\Delta_f H^\circ(ONOO^-) = -10 \pm 1$ kcal/mol[51] and $\Delta H^\circ = 4 \pm 2$ kcal/mol[22] were reported for the acidic dissociation of ONOOH. The latter value was confirmed by us, and we obtained 4.3 ± 0.5 kcal/mol. Thus, $\Delta_f H^\circ(ONOOH) = -14.3 \pm 1$ kcal/mol. Furthermore, $\Delta_f H^\circ(^\bullet NO_2) = 2.9$ kcal/mol.[52] The enthalpy of formation of $^\bullet OH$(aq) can be estimated as follows. Comparing the entropies of hydration of gaseous Ne, N_2, CO, O_2, H_2O, and H_2O_2,[53] we find that they all lie between −19 and −25 eu. It is therefore reasonable to assume the corresponding value for $^\bullet OH$ to be -22 ± 3 eu. As $S^\circ(^\bullet OH, gas) = 44$ eu, this yields $S^\circ(^\bullet OH, aq) = 22 \pm 3$ eu. Thus, $\Delta_f H^\circ(^\bullet OH, aq) = 0.8 \pm 1$ kcal/mol is calculated from $\Delta_f G^\circ(^\bullet OH, aq) = 6.2$ kcal/mol[44] and $S^\circ(^\bullet OH, aq) = 22 \pm 3$ eu. Combining the relevant $\Delta_f H^\circ$ values, we obtain $\Delta H^\circ_1 = 18 \pm 2$ kcal/mol, in excellent agreement with the one derived from the activation energy.

The enthalpy of dissociation of $^\bullet OH$ into $O^{\bullet -}$ and H^+ has been reported to be 10 ± 2 kcal/mol.[54] The lower limit of 8 kcal/mol appears more reasonable than the average value, given that the enthalpy of dissociation of H_2O_2 is 7.4 kcal/mol, and $pK_a(H_2O_2) = 11.7$ is almost the same as $pK_a(^\bullet OH) = 11.9$. Therefore, a value of 8 ± 2 kcal/mol for the enthalpy of $^\bullet OH$ dissociation was adopted, which together with $\Delta_f H^\circ(^\bullet OH, aq) = 0.8$ kcal/mol yields $\Delta_f H^\circ(O^{\bullet -}, aq) = 8.8 \pm 2$ kcal/mol. Utilizing this value together with $\Delta_f H^\circ(^\bullet NO_2) = 2.9$ kcal/mol and $\Delta_f H^\circ(ONOO^-) = -10$ kcal/mol, we obtain $\Delta H^\circ_3 = 21.7 \pm 3$ kcal/mol. Within the error limit this value compares favorably to the activation energy of reaction 3, $(E_a)_3 = 21.7 \pm 0.5$ kcal/mol. In conclusion, the description of the ONOOH/$ONOO^-$ system in terms of radical homolysis and subsequent radical reactions explains fully the experimental results and is essentially complete.

Acknowledgment. G.M. and J.L. thank the Swedish Natural Science Research Council and S.G. and G.C. the Israel Science Foundation for their financial support.

References and Notes

(1) Beckman, J. S.; Beckman, T. W.; Chen, J.; Marshall, P. A.; Freeman, B. A. *Proc. Natl. Acad. Sci. U.S.A.* **1990**, *87*, 1620.

(2) Huie, R. E.; Padmaja, S. *Free Rad. Res. Commun.* **1993**, *18*, 195.

(3) Goldstein, S.; Czapski, G. *Free Rad. Biol. Med.* **1995**, *19*, 505.

(4) Kobayashi, K.; Miki, M.; Tagawa, S. *J. Chem. Soc., Dalton Trans.* **1995**, 2885.

(5) Kissner, R.; Nauser, T.; Bugnon, P.; Lye, P. G.; Koppenol, W. H. *Chem. Res. Toxicol.* **1997**, *10*, 87.

(6) The experiments in refs 2−4 are essentially equivalent, in that all three produce $O_2^{\bullet -}$ from formate and O_2 and $^\bullet NO$ from NO_2^-, whereupon $^\bullet NO$ and $O_2^{\bullet -}$ recombine to yield $ONOO^-$. In ref 2 equal amounts of $O_2^{\bullet -}$, and $^\bullet NO$ are formed simultaneously and the combination occurs without delay in a second-order process. In refs 3 and 4 pseudo-first-order conditions prevail with $[O_2^{\bullet -}]/[^\bullet NO] > 1$. As $^\bullet NO$ is produced from a precursor, NO_2^{2-}, there is, in principle, a slight delay between radical production and combination. However, in practice, both systems contain high amounts of phosphate buffer, which catalyzes very efficiently the conversion of NO_2^{2-} into $^\bullet NO$, and the latter process does not interfere with the coupling reaction of $^\bullet NO$ with $O_2^{\bullet -}$ to yield $ONOO^-$. Equally important, the measured rate constants in the three papers 2−4 agree within better than a factor of 2. Reference 5 utilizes photochemical bleaching and restoration of the $ONOO^-$ absorbance. In principle, this method should provide the cleanest route for the determination of $k(^\bullet NO + O_2^{\bullet -})$, provided that no other species except $^\bullet NO + O_2^{\bullet -}$ are formed during photolysis. This point has not been dealt with satisfactorily in ref 5. In particular, the reported formation of gas bubbles after 800 flashes, which are not expected to be seen after one flush,

indicates that $ONOO^-$ may have split into $^{\bullet}NO_2 + {}^{\bullet}OH/O^{\bullet-}$ or $NO^- + O_2$ to some extent.

(7) Pryor, W. A.; Squadrito, G. L. *Am. J. Physiol*. **1995**, *268*, L699.

(8) Logager, T.; Sehested, K. *J. Phys. Chem*. **1993**, *97*, 6664.

(9) Papée, H. M.; Petriconi, G. L. *Nature (London)* **1964**, *204*, 142.

(10) Petriconi, G. L.; Papée, H. M. *J. Inorg. Nucl. Chem.* **1968**, *30*, 1525.

(11) Keith, W. G.; Powell, R. E. *J. Chem. Soc. A* **1969**, 90.

(12) Hughes, M. N.; Nicklin, H. G. *J. Chem. Soc. A* **1970**, 925.

(13) Hughes, M. N.; Nicklin, H. G.; Sackrule, N. A. C. *J. Chem. Soc. A* **1971**, 3722.

(14) Edwards, J. O.; Plumb, R. C. *Prog. Inorg. Chem*. **1993**, *41*, 599.

(15) Lymar, S. V.; Hurst, J. K. *J. Am. Chem. Soc.* **1995**, *117*, 8867.

(16) Goldstein, S.; Czapski, G. *J. Am. Chem. Soc.* **1998**, *120*, 3458.

(17) Lymar, S. V.; Hurst, J. K. *Inorg. Chem.* **1998**, *37*, 294.

(18) Pfeiffer, S.; Gorren, A. C. F.; Schmidt, K.; Werner, E. R., Hansert, B.; Bohle, D. S.; Mayer, B. *J. Biol. Chem.* **1997**, *272*, 3465.

(19) Lymar, S. V.; Hurst, J. K. *Chem. Res. Toxicol*. **1998**, *11*, 714.

(20) Goldstein, S.; Squadrito, G. L.; Pryor, W. A.; Czapski, G. *Free Rad. Biol. Med.* **1996**, *21*, 965.

(21) Merényi, G.; Lind, J. *Chem. Res. Toxicol*. **1997**, *10*, 1216.

(22) Koppenol, W. H.; Kissner, R. *Chem. Res. Toxicol*. **1998**, *11*, 87.

(23) Marnett, L. J. *Chem. Res. Toxicol*. **1998**, *11*, 1. Forum: Reactive Species of Peroxynitrite.

(24) Merényi, G.; Lind, G. *Chem. Res. Toxicol*. **1998**, *11*, 243.

(25) Koppenol, W. H. J.; Moreno, J. J.; Pryor, W. A.; Ischiropoulos, H.; Beckman, J. S. *Chem. Res. Toxicol.* **1992**, *4*, 834.

(26) Padmaja, S.; Kissner, R.; Bounds, P. L.; Koppenol, W. H. *Helv. Chim. Acta* **1998**, *81*, 1201.

(27) Merényi, G.; Lind, G.; Goldstein, S.; Czapski, G. *Chem. Res. Toxicol*. **1988**, *11*, 712.

(28) Saha, A.; Goldstein, S., Cabelli, D.; Czapski, G. *Free Rad. Biol. Med.* **1998**, *24*, 653.

(29) Hughes, M. N.; Nicklin, H. G. *J. Chem. Soc. A* **1968**, 450.

(30) Eriksen, T. E.; Lind, J.; Reitberger, T. *Chem. Scr.* **1976**, *10*, 5.

(31) Buxton, G. V.; Stuart, C. R. *J. Chem. Soc., Faraday Trans.* **1995**, *91*, 279.

(32) Mallard, W. G.; Ross, A. B.; Helman, W. P. *NIST Standard References Database 40, Version 3.0*, 1998.

(33) The yield of ferricyanide was measured at 420 nm upon pulse irradiation of N_2O-saturated solutions ($[N_2O] \approx 25$ mM) containing 0.5 mM ferrocyanide and 0−2 mM nitrite at pH 8 (2 mM phosphate buffer). Ferricyanide is formed due to the fast reaction of $^{\bullet}OH$ radicals with ferrocyanide ($k = 1.1 \times 10^{10}$ M^{-1} s^{-1}).[32] The 10% $H^{\bullet}$ radicals formed by the radiation react partly with N_2O ($k = 2.1 \times 10^6$ M^{-1} s^{-1})[32] to yield $^{\bullet}OH$ and partly reduce ferricyanide ($k = 6.3 \times 10^9$ M^{-1} s^{-1}).[32] Therefore, the yield of ferricyanide approximates well the yield of $^{\bullet}OH$ radicals formed by the radiation as confirmed by measuring the same absorption 5 μs and 40 ms after the pulse. Nitrite competes with ferrocyanide for $^{\bullet}OH$ and scavenges the $H^{\bullet}$ radicals due to reaction 11. Hence, ferricyanide is formed via the oxidation of ferrocyanide by both $^{\bullet}OH$ and $^{\bullet}NO_2$, which are two well-separated processes.[32] The rate of the second slow process was independent of nitrite concentration, $k_{obs} = (1.2 \pm 0.1) \times 10^3$ s^{-1}, which agrees well with the literature value for $k(^{\bullet}NO_2 + Fe(CN)_6^{4-})$.[32] The reciprocal yield of ferricyanide due to the reaction of $^{\bullet}OH$ with ferrocyanide was linearly dependent on $[NO_2^-]_o$, resulting in $k_4 = (5.3 \pm 0.5) \times 10^9$ M^{-1} s^{-1}.

(34) Gerasimov, O.; Lymar, S. G. Private communication. N_2O-saturated solutions containing $IrCl_6^{3-}$ at pH 5.7 (63 mM phosphate) were pulse-irradiated and the yield of $IrCl_6^{2-}$ was measured in the presence of various concentrations of nitrite. The competition plot results $k_4 = (7.3 \pm 0.5) \times 10^9$ M^{-1} s^{-1} using $k(^{\bullet}OH + IrC_6^{3-}) = (1.2 \pm 0.1) \times 10^{10}$ M^{-1} s^{-1}.

(35) Goldstein, S.; Saha, A.; Lymar, S.; Czapski, G. *J. Am. Chem. Soc*. **1998**, *120*, 5549.

(36) Graetzel, M.; Henglein, A.; Lilie, J.; Beck, G. *Ber. Bunsen-Ges. Phys. Chem*. **1969**, *73*, 646.

(37) One of the referees pointed out that $k_{10} \approx 2 \times 10^{10}$ M^{-1} s^{-1} and, if $k_{10} = 7 \times 10^9$ M^{-1} s^{-1} as reported,[32] the radical yields in acid solution would be about 50% larger than found.

(38) Computer modeling of the experimental yields of peroxynitrite as reported in ref 8, using our reaction mechanism, yields $k_{-1} = (4-6) \times 10^9$ M^{-1} s^{-1} for 0.1−1 mM nitrite. For 50 μM nitrite k_{-1} exceeds 8×10^9 M^{-1} s^{-1}.

(39) Graetzel, M.; Taniguchi, S.; Henglein, A. *Ber. Bunsen-Ges. Phys. Chem*. **1970**, *74*, 292.

(40) Under the experimental conditions given in ref 8 (pH 0−3.85, $[NO_3^-] = 1$ mM), H^+ competes efficiently with NO_3^- for e_{aq}^- to yield $H^{\bullet}$ with $k = 2.3 \times 10^{10}$ M^{-1} s^{-1}, and the latter disappears mainly via reactions 9 and 10, where reaction 10 was ignored in ref 8. We simulated the yield of ONOOH using the reaction mechanism given in ref 8 ($k_{-1} = 4.5 \times 10^9$ M^{-1} s^{-1}, $k_{10} = 0$) and were able to fit the calculated yields to the reported experimental ones only at pH 3.85. We repeated this experiment at pH 3.9 (2 mM nitrate, 39 Gy/pulse), where 87% of e_{aq}^- are scavenged by nitrate. The yield of ONOOH was measured at 270 nm ($\epsilon = 450$ M^{-1} cm^{-1})[8] to be 2.4 ± 0.3 μM. The calculated yields of ONOOH obtained via simulations (including reaction 10) for $k_{-1} = 5 \times 10^9$ M^{-1} s^{-1} and $k_{-1a} = 0$ or 5×10^9 M^{-1} s^{-1} are 4.0 and 2.6 μM, respectively. We therefore conclude that our result at pH 3.9 is in agreement with $k_{-1} \approx k_{-1a} = 5 \times 10^9$ M^{-1} s^{-1}, and we have no explanation for the reported high yields in ref 8.

(41) Logager, T.; Sehested, K. *J. Phys. Chem*. **1993**, *97*, 10047.

(42) Goldstein, S.; Czapski, G.; Lind, J.; Merényi, G. *Inorg. Chem*. **1998**, *37*, 3943.

(43) Of special interest are the reactions of reducing carbon-centered radicals, such as α-hydroxy and α-alkoxy alkyl radicals with ONOOH. The latter radicals are produced when, e.g., $^{\bullet}OH$ abstracts hydrogen from alcohols and ethers, sometimes added as $^{\bullet}OH$ scavengers to ONOOH-containing systems. While such reactions have not been investigated with ONOOH as a substrate, it is known that alkyl radicals react fast with peroxycarboxylic acids via OH transfer (this is the propagation step during the chain conversion of peroxycarboxylic acids to alcohols), and the reaction is faster the lower the ionization potential of the alkyl radical (see, e.g., Fossey, J.; Lefort, D. *Tetrahedron* **1980**, *36*, 1023).

(44) Stanbury, D. M. *Adv. Inorg. Chem*. **1989**, *33*, 69.

(45) Elliot, A. J.; McCracken, D. R. *Radiat. Phys. Chem*. **1989**, *33*, 69.

(46) We assume that the rate constant is similar to that determined for the reaction of $^{\bullet}NO$ with $CO_3^{\bullet-}$ by: Czapski, G.; Holcman, J.; Bielski, B. H. J. *J. Am. Chem. Soc*. **1994**, *116*, 11465.

(47) Treinin, A.; Hayon, E. *J. Am. Chem. Soc*. **1970**, *92*, 5821.

(48) Rabinowitch, E.; Wood, W. C. *Trans. Faraday Soc*. **1937**, *33*, 1225.

(49) Lampe, F. W.; Noyes, R. M. *J. Am. Chem. Soc*. **1954**, *76*, 2140.

(50) Koenig, T. In *Free Radicals*; Kochi, J. K., Eds.; John Wiley & Sons: New York, 1973; Vol. 1, Chapter 3, pp 112−155.

(51) Manuszak, M.; Koppenol, W. H. *Thermochim. Acta* **1996**, *273*, 11.

(52) Mertes, S.; Wahner, A. *J. Phys. Chem*. **1995**, *99*, 14000.

(53) O'Sullivan, D. W.; Lee, M.; Noone, B. C.; Heikes, B. G. *J. Phys. Chem*. **1996**, *100*, 3241.

(54) Baxendale, J. H.; Ward, M. D.; Wardman, P. *Trans. Faraday Soc*. **1971**, *67*, 2532.